Inclusive production of $f_2(1270)$ tensor mesons at the LHC via gluon-gluon fusion in the k_t-factorization approach

A. Szczurek[†,∗] and P. Lebiedowicz

Institute of Nuclear Physics Polish Academy of Sciences,
Radzikowskiego 152, PL-31342 Kraków, Poland

E-mail: Antoni.Szczurek@ifj.edu.pl, Piotr.Lebiedowicz@ifj.edu.pl

The cross section for inclusive production of $f_2(1270)$ meson is calculated. We include both the mechanism of gluon-gluon fusion as well as the $\pi\pi$ final-state rescattering. The contribution of the gluon-gluon fusion is calculated within the k_t-factorization approach with modern unintegrated gluon distribution functions (UGDFs). Some parameters for the $g^*g^* \to f_2$ vertex are extracted from the $\gamma\gamma \to f_2(1270) \to \pi\pi$ reactions. The results strongly depend on the parametrization of the $g^*g^* \to f_2(1270)$ form factor. Results of our model are compared to the ALICE preliminary data. The gluon-gluon fusion does not explain low-p_t data but could be the dominant mechanism at somewhat larger meson transverse momenta. By adjusting some parameters the pion-pion rescattering can explain the low-p_t region.

∗Speaker

†Also at *College of Natural Sciences, Institute of Physics, University of Rzeszów, Pigonia 1, PL-35310 Rzeszów, Poland.*

1. Introduction

The mechanism of f_2(1270) meson production in proton-proton collisions is not well understood. For instance in event generators f_2(1270) is not produced in a primary fragmentation process but occurs only in decays. The f_2(1270) is also difficult to observe experimentally. The dominant decay channel is $f_2(1270) \to \pi^+\pi^-$. Only STAR [1] and ALICE [2] undertook experimental efforts.

The gluon-gluon fusion was already considered in the past [3]. Recently [4] we discussed this mechanism more carefully.

In figure 1 we show a Feynman diagram for the f_2(1270) meson production via gluon-gluon fusion in proton-proton collisions.
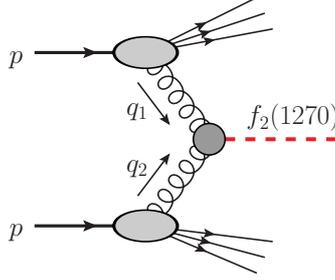

Figure 1: General diagram for inclusive f_2(1270) production via gluon-gluon fusion in *pp* collisions.

We applied k_t-factorization approach used by our group for χ_c quarkonium production [5, 6], for $\eta_c(1S, 2S)$ production [7, 8], and also for f_0(980) production [9]. The colour singlet gluon-gluon fusion is similar to photon-photon fusion discussed e.g. in [10]. There two tensor structures corresponding to $\Gamma^{(0)}$ helicity-0 and $\Gamma^{(2)}$ helicity-2 couplings were found and their strength was determined from the comparison to the Belle data [11] for the $\gamma\gamma \to \pi\pi$ reactions. In [4] we also used tensorial structures for $\gamma^*\gamma^* \to f_2$(1270) vertex from [12].

2. Model calculations

In [10] the $f_2\gamma\gamma$ vertex for 'on-shell' f_2 meson and real photons was considered; see (3.39) of [10] and the discussion in section 5.3 there. In [4] we were interested in $\gamma^*(Q_1^2)\gamma^*(Q_2^2) \to f_2$(1270) process. Thus to describe the dependence on photon virtualities we introduced the vertex form factors $F^{(0)}(Q_1^2, Q_2^2)$ and $F^{(2)}(Q_1^2, Q_2^2)$.

Then the $\gamma^*\gamma^* \to f_2$(1270) vertex, including the form factors $F^{(\Lambda)}$ (for $\Lambda = 0, 2$) were parametrized as

$$\Gamma_{\mu\nu\kappa\lambda}^{(f_2\gamma\gamma)}(q_1, q_2) = 2a_{f_2\gamma\gamma}\, \Gamma_{\mu\nu\kappa\lambda}^{(0)}(q_1, q_2)\, F^{(0)}(Q_1^2, Q_2^2) - b_{f_2\gamma\gamma}\, \Gamma_{\mu\nu\kappa\lambda}^{(2)}(q_1, q_2)\, F^{(2)}(Q_1^2, Q_2^2), \quad (1)$$

with two rank-four tensor functions $\Gamma^{(0)}$ and $\Gamma^{(2)}$ (see (3.18)–(3.22) of [10]).

To obtain $a_{f_2\gamma\gamma}$ and $b_{f_2\gamma\gamma}$ in (1) we used the experimental value of the radiative decay width

$$\Gamma(f_2 \to \gamma\gamma) = (2.93 \pm 0.40)\,\text{keV}\,,$$
$$\text{helicity zero contribution} \approx 9\% \text{ of } \Gamma(f_2 \to \gamma\gamma)\,, \quad (2)$$

as quoted for the preferred solution III in Table 3 of [11]. Using the decay rate from (5.28) of [10]

$$\Gamma(f_2 \to \gamma\gamma) = \frac{m_{f_2}}{80\pi}\left(\frac{1}{6}m_{f_2}^6|a_{f_2\gamma\gamma}|^2 + m_{f_2}^2|b_{f_2\gamma\gamma}|^2\right) \quad (3)$$

and assuming $a_{f_2\gamma\gamma} > 0$ and $b_{f_2\gamma\gamma} > 0$, we find $a_{f_2\gamma\gamma} = \alpha_{\mathrm{em}} \times 1.17$ GeV^{-3} and $b_{f_2\gamma\gamma} = \alpha_{\mathrm{em}} \times 2.46$ GeV^{-1}, where $\alpha_{\mathrm{em}} = e^2/(4\pi) \simeq 1/137$.

It was shown in Refs. [12–14] that the most general amplitude for the process $\gamma^*(q_1, \lambda_1) + \gamma^*(q_2, \lambda_2) \rightarrow f_2(\Lambda)$, describing the transition from two virtual photons to a tensor meson f_2 ($J^{PC} = 2^{++}$) with the mass m_{f_2} and helicity $\Lambda = \pm2, \pm1, 0$, involves five independent structures.

In the formalism in [12] the $\gamma^*\gamma^* \rightarrow f_2(1270)$ vertex was parameterized as

$$
\begin{aligned}
\Gamma^{(f_2\gamma\gamma)}_{\mu\nu\kappa\lambda}(q_1, q_2) = 4\pi\alpha_{\mathrm{em}} &\left\{ \left[R_{\mu\kappa}(q_1, q_2) R_{\nu\lambda}(q_1, q_2) + \frac{s}{8X} R_{\mu\nu}(q_1, q_2)(q_1 - q_2)_\kappa (q_1 - q_2)_\lambda \right] \right. \\
&\times \frac{\nu}{m_{f_2}} T^{(2)}(Q_1^2, Q_2^2) \\
&+ R_{\nu\kappa}(q_1, q_2)(q_1 - q_2)_\lambda \left(q_{1\mu} + \frac{Q_1^2}{\nu} q_{2\mu} \right) \frac{1}{m_{f_2}} T^{(1)}(Q_1^2, Q_2^2) \\
&+ R_{\mu\kappa}(q_1, q_2)(q_2 - q_1)_\lambda \left(q_{2\nu} + \frac{Q_2^2}{\nu} q_{1\nu} \right) \frac{1}{m_{f_2}} T^{(1)}(Q_2^2, Q_1^2) \\
&+ R_{\mu\nu}(q_1, q_2)(q_1 - q_2)_\kappa (q_1 - q_2)_\lambda \frac{1}{m_{f_2}} T^{(0,\mathrm{T})}(Q_1^2, Q_2^2) \\
&\left. + \left(q_{1\mu} + \frac{Q_1^2}{\nu} q_{2\mu} \right) \left(q_{2\nu} + \frac{Q_2^2}{\nu} q_{1\nu} \right) (q_1 - q_2)_\kappa (q_1 - q_2)_\lambda \frac{1}{m_{f_2}^3} T^{(0,\mathrm{L})}(Q_1^2, Q_2^2) \right\},
\end{aligned}
\tag{4}
$$

where photons with four-momenta q_1 and q_2 have virtualities, $Q_1^2 = -q_1^2$ and $Q_2^2 = -q_2^2$, $s = (q_1 + q_2)^2 = 2\nu - Q_1^2 - Q_2^2$, $X = \nu^2 - q_1^2 q_2^2$, $\nu = (q_1 \cdot q_2)$, and

$$
R_{\mu\nu}(q_1, q_2) = -g_{\mu\nu} + \frac{1}{X} \left[\nu \left(q_{1\mu} q_{2\nu} + q_{2\mu} q_{1\nu} \right) - q_1^2 q_{2\mu} q_{2\nu} - q_2^2 q_{1\mu} q_{1\nu} \right].
\tag{5}
$$

In (4) $T^{(\Lambda)}(Q_1^2, Q_2^2)$ are the $\gamma^*\gamma^* \rightarrow f_2(1270)$ transition form factors for $f_2(1270)$ helicity Λ. For the case of helicity zero, there are 2 form factors depending on whether both photons are transverse (T) or longitudinal (L). We express the transition form factors as

$$
T^{(\Lambda)}(Q_1^2, Q_2^2) = F^{(\Lambda)}(Q_1^2, Q_2^2) T^{(\Lambda)}(0, 0).
\tag{6}
$$

In the limit $Q_{1,2}^2 \rightarrow 0$ only $T^{(0,\mathrm{T})}$ and $T^{(2)}$ contribute and their values at $Q_{1,2}^2 \rightarrow 0$ determine the two-photon decay width of $f_2(1270)$ meson.

Comparing two approaches, EMN and PPV, given by (1) and (4)–(6), respectively, at both real photons ($Q_1^2 = Q_2^2 = 0$) and at $\sqrt{s} = m_{f_2}$ we found the correspondence

$$
4\pi\alpha_{\mathrm{em}} T^{(0,\mathrm{T})}(0, 0) = -a_{f_2\gamma\gamma} \frac{m_{f_2}^3}{2},
\tag{7}
$$

$$
4\pi\alpha_{\mathrm{em}} T^{(2)}(0, 0) = -b_{f_2\gamma\gamma} 2m_{f_2}.
\tag{8}
$$

The $g^*g^* \rightarrow f_2(1270)$ coupling entering in the matrix element squared was obtained from that for the $\gamma^*\gamma^* \rightarrow f_2(1270)$ coupling by the following replacement:

$$
\alpha_{\mathrm{em}}^2 \rightarrow \alpha_{\mathrm{s}}^2 \frac{1}{4N_c(N_c^2 - 1)} \frac{1}{(< e_q^2 >)^2}.
\tag{9}
$$

Above $(< e_q^2 >)^2 = 25/162$ for the $\frac{1}{\sqrt{2}} \left(u\bar{u} + d\bar{d} \right)$ flavour structure assumed for $f_2(1270)$.

The running of strong coupling constants was included. In numerical calculations the renormalization scale was taken in the form:

$$\alpha_s^2 \rightarrow \alpha_s(\max\{m_T^2, \boldsymbol{q}_1^2\}) \, \alpha_s(\max\{m_T^2, \boldsymbol{q}_2^2\}) \,. \tag{10}$$

The Shirkov-Solovtsov prescription [15] is used to extrapolate down to small renormalization scales relevant for the $f_2(1270)$ production for the ALICE kinematics.

Because $f_2(1270)$ is extended, finite size object one can expect in addition a form factor $F(Q_1^2, Q_2^2)$ associated with the gluon virtualities for the $g^*g^* \rightarrow f_2$ vertex. In [4] the form factor was parametrized in four different ways; see (2.13)–(2.16) of [4].

3. Comparison to ALICE data

In [4] we showed our results to the ALICE data presented in a PhD thesis [2]. To convert to the number of $f_2(1270)$ mesons per event we used the relation:

$$\frac{dN}{dp_t} = \frac{1}{\sigma_{\text{inel}}} \frac{d\sigma}{dp_t} \,. \tag{11}$$

The inelastic cross section for $\sqrt{s} = 7$ TeV was obtained by the TOTEM [17] and ATLAS [18] collaborations. In our calculations we took $\sigma_{\text{inel}} = 72.5$ mb.

In figure 2 we present the $f_2(1270)$ meson transverse momentum distributions at $\sqrt{s} = 7$ TeV and $|y| < 0.5$ together with the preliminary ALICE data. Here, for the color-singlet gluon-gluon fusion mechanism, we used JH UGDF from [19]. We compare results for the monopole and dipole form factors for two different $g^*g^* \rightarrow f_2$ vertices.
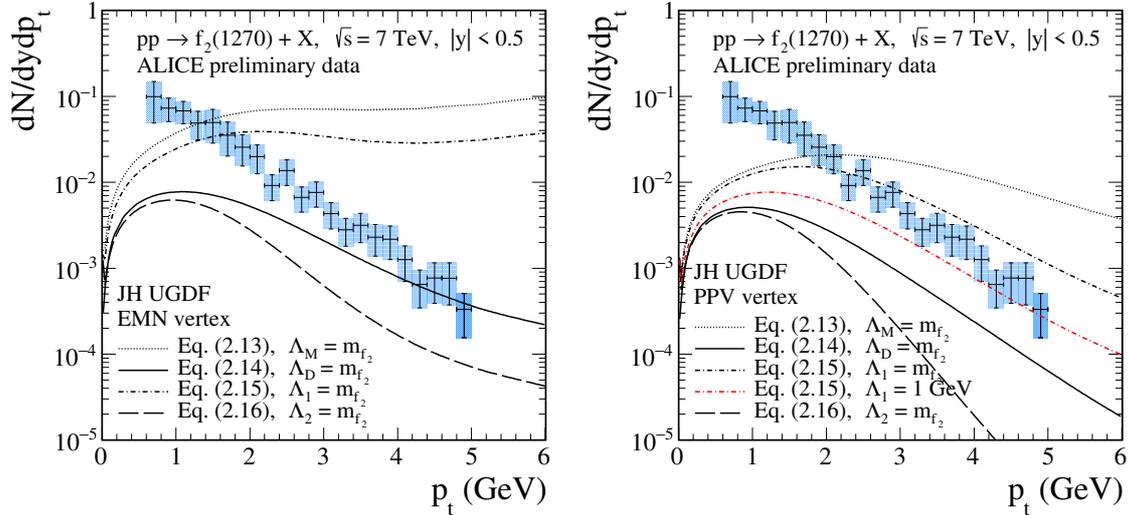

Figure 2: The $f_2(1270)$ meson transverse momentum distributions at $\sqrt{s} = 7$ TeV and $|y| < 0.5$. The preliminary ALICE data from [2] are shown for comparison. The results for the EMN (left panel) and PPV (right panel) $g^*g^* \rightarrow f_2(1270)$ vertex for different $F(Q_1^2, Q_2^2)$ form factor (2.13)–(2.16) from [4] are shown. In this calculation the JH UGDF was used.

In the formalism of [12] [see the PPV vertex (4)] there is no interference between $\Lambda = 0, T$ and $\Lambda = 2$ terms while the naive use of the formalism from [10] [see the EMN vertex (1)] generates some interference effects. Different couplings lead to different shapes of the transverse momentum distributions; see [4] for details and more results.

In the left panel of figure 3 we show results for the KMR UGDF. Here we use a glue constructed according to the prescription initiated in [21] and later updated in [22], which we label as "KMR UGDF". The KMR UGDF is available from the CASCADE Monte Carlo code [20]. The KMR UGDF (dashed lines) gives smaller cross section than the JH UGDF (solid lines). The results for both UGDFs coincide for large p_t. The larger the $f_2(1270)$ transverse momentum the larger the range of gluon transverse momenta q_{1t} and/or q_{2t} are probed. In the right panel of figure 3 we show the $\pi\pi$-rescattering contribution. In the $\pi\pi$-rescattering mechanism we used a Lévy parametrization of the inclusive π^0 cross section proposed in [16] for $\sqrt{s} = 7$ TeV; see [4] for details. Clearly the $\pi\pi \to f_2(1270)$ rescattering effect cannot describe the region of $p_t > 2$ GeV, where the gg-fusion mechanism is a possible explanation.
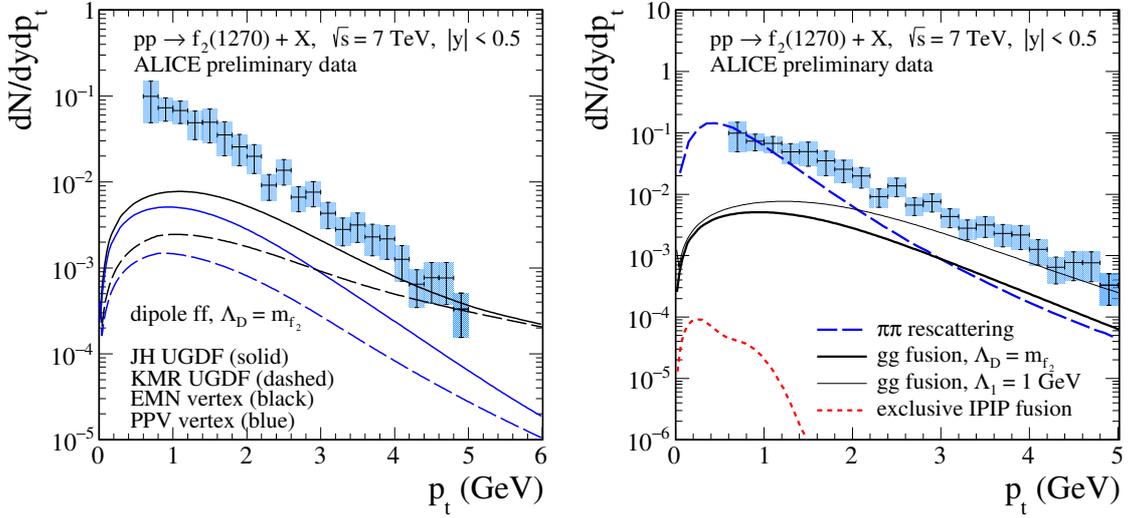

Figure 3: In the left panel results for two different UGDFs, JH (solid lines) and KMR (dashed lines), together with the preliminary ALICE data from [2] are shown. In the right panel results for the $\pi\pi$ rescattering mechanism (long-dashed line), for the gg-fusion (JH UGDF) mechanism (solid lines), and for the pomeron-pomeron fusion mechanism (dotted line) are shown. The dotted (red) line corresponds to the Born-level result for the exclusive $pp \to pp f_2(1270)$ reaction via pomeron-pomeron fusion; see [23, 24].

4. Conclusions

In this presentation results obtained in [4] have been presented. Two different approaches for the $g^*g^* \to f_2(1270)$ coupling were considered. The coupling constants have been fixed by the Belle data for $\gamma\gamma \to f_2(1270) \to \pi\pi$. Then, the $g^*g^* \to f_2(1270)$ vertices have been obtained by replacing electromagnetic coupling constant by the strong coupling constant, modifying color factors and assuming a simple flavour structure of the $f_2(1270)$ isoscalar meson.

Our calculation of the cross section for $pp \to f_2(1270) + X$ were performed within the k_t-factorization approach using different unintegrated gluon distributions.

5

At low f_2(1270) transverse momenta the helicity-2 ($\Lambda = 2$) contribution dominates, while the helicity-0 ($\Lambda = 0$, T) is small. However, the latter competes with the $\Lambda = 2$ contribution at larger transverse momenta of f_2(1270). In the PPV formalism there are also $\Lambda = 0$, L and $\Lambda = 1$ contributions which are, however, difficult to fix at present.

It has been shown that the results strongly depend on the form of the vertex form factor which is poorly known at present. While one can describe the data for $p_t > 2$ GeV, it seems impossible to describe the low-p_t data. We have shown that there one may expect $\pi\pi$ rescattering. Adjusting one parameter of a simple model for the $\pi\pi$ rescattering one can describe the region of small p_t.

Acknowledgments

References

[1] J. Adams *et al.*, (STAR Collaboration), Phys. Rev. Lett. **92** (2004) 092301.

[2] G. R. Lee, Ph.D. thesis: *Resonance production in the $\pi^+\pi^-$ decay channel in proton-proton collisions at 7 TeV*, University of Birmingham, 2016. http://www.hep.ph.bham.ac.uk/publications/thesis/grl_thesis.pdf

[3] F. Fillion-Gourdeau and S. Jeon, Phys. Rev. **C77** (2008) 055201.

[4] P. Lebiedowicz and A. Szczurek, Phys. Lett. **B810** (2020) 135816.

[5] A. Cisek and A. Szczurek, Phys. Rev. **D97** (2018) 034035.

[6] I. Babiarz, R. Pasechnik, W. Schäfer, and A. Szczurek, JHEP **06** (2020) 101.

[7] S. P. Baranov and A. V. Lipatov, Eur. Phys. J. **C79** (2019) 621.

[8] I. Babiarz, R. Pasechnik, W. Schäfer, and A. Szczurek, JHEP **02** (2020) 037.

[9] P. Lebiedowicz, R. Maciuła, and A. Szczurek, Phys. Lett. B **806** (2020) 135475.

[10] C. Ewerz, M. Maniatis, and O. Nachtmann, Annals Phys. **342** (2014) 31.

[11] L.-Y. Dai and M. R. Pennington, Phys.Rev. D **90** (2014) 036004.

[12] V. Pascalutsa, V. Pauk, and M. Vanderhaeghen, Phys. Rev. **D85** (2012) 116001.

[13] M. Poppe, Int. J. Mod. Phys. **A1** (1986) 545.

[14] G. A. Schuler, F. A. Berends, and R. van Gulik, Nucl. Phys. B **523** (1998) 423.

[15] D. V. Shirkov and I. L. Solovtsov, Phys. Rev. Lett. **79** (1997) 1209.

[16] B. Abelev *et al.*, (ALICE Collaboration), Phys. Lett. **B717** (2012) 162.

[17] G. Antchev *et al.*, (TOTEM Collaboration), EPL **101** (2013) 21002.

[18] G. Aad *et al.*, (ATLAS Collaboration), Nucl. Phys. **B889** (2014) 486.

[19] F. Hautmann and H. Jung, Nucl. Phys. **B883** (2014) 1.

[20] H. Jung *et al.*, Eur. Phys. J. **C70** (2010) 1237.

[21] M. A. Kimber, A. D. Martin, and M. G. Ryskin, Phys. Rev. **D63** (2001) 114027.

[22] A. D. Martin, M. G. Ryskin, and G. Watt, Eur. Phys. J. **C66** (2010) 163.

[23] P. Lebiedowicz, O. Nachtmann, and A. Szczurek, Phys. Rev. **D93** (2016) 054015.

[24] P. Lebiedowicz, O. Nachtmann, and A. Szczurek, Phys. Rev. D **101** (2020) 034008.